Energy and Buildings 68 (2014) 33–41

Contents lists available at ScienceDirect

Energy and Buildings

journal homepage: www.elsevier.com/locate/enbuild

Experimental study of melting and solidification of PCM in a triplex tube heat exchanger with fins

Abduljalil A. Al-Abidi [a,b,*], Sohif Mat [a], K. Sopian [a], M.Y. Sulaiman [a], Abdulrahman. Th. Mohammad [a]

[a] Solar Energy Research Institute, University Kebangsaan Malaysia, Bangi, Selangor, Malaysia
[b] Department of HVAC Engineering, Sana'a Community College, P.O. Box 5695 Sana'a, Yemen

ARTICLE INFO

Article history:
Received 10 April 2013
Received in revised form 9 July 2013
Accepted 3 September 2013

Keywords:
Melting
Solidification
Thermal energy storage
PCM
Triplex tube heat exchanger

ABSTRACT

Thermal energy storage improves the efficiency and eliminates the mismatch between the energy supply and energy demand of solar thermal energy applications. Among the different types of thermal energy storage, a phase change material (PCM) thermal energy storage exhibits superior efficiency and dependability due to its high storage capacity and nearly constant thermal energy. The present work experimentally investigates the use of a triplex tube heat exchanger with internal–external fins as thermal energy storage. The experiment examined the PCM charging process under steady and non-steady heat transfer fluid (HTF) inlet temperature and the influence of the mass flow rates on the PCM melting. The PCM solidification process under different mass flow rates was also investigated, and the PCM temperature gradients in the radial and angular directions were analyzed. The results indicated that the HTF inlet temperature has more influence on the PCM melting process than the HTF mass flow rate. The charging time is reduced to 58% for HTF mass flow rate and 86% for HTF inlet temperature.

1. Introduction

The drawback of the phase change materials (PCMs) is its low thermal conductivity, an inferior property that hinders the application of these materials for thermal energy storage. It prolongs the charging and discharging process of the thermal energy storage. For over three decades, researchers have comprehensively studied the heat transfer enhancement of the PCM thermal storage. Their studies investigated different techniques to improve the heat transfer between the PCM and the heat transfer fluid (HTF). These techniques are implemented either by increasing the heat transfer area (e.g., utilization of finned tubes [1], application of multitubes heat exchangers [2], and using heat pipes [3]) or improving the PCM thermal conductivity (e.g., insertion of metal matrix into the PCM, impregnation of porous materials, utilization of bubble agitation in the PCMs [4], and application of PCM dispersed with high conductivity particles [5]). The other enhancement method for the heat transfer process by maintaining a constant temperature difference between the PCM and the HTF involves the use of multiple families of PCMs, which are packed in the decreasing order of their melting points in the flow direction of the thermal storage [6,7].

The PCM thermal energy storage can improve energy efficiency while minimizing the mismatch between the energy supply and demand. Compared with the sensible energy storage, this latent heat thermal energy storage exhibits superior efficiency and dependability because of its high storage capacity and nearly constant thermal energy [8]. Numerous authors have studied the PCM thermal characteristic during charging and discharging processes in energy storage systems. Farid et al. [9] presented a review on the investigation of PCM materials, encapsulation and applications. Hu and Argyropoulos [10] performed a review of mathematical modeling methods of solidification and melting. Khudhair and Farid [11] carried out the investigation and analysis of thermal energy storage systems incorporating PCMs for use in building applications. PCMs are used in various engineering applications such as thermal energy storage in building structures and equipment [12], including domestic hot water, heating and cooling systems, electronic products, drying technology, waste heat recovery, refrigeration and cold storage, solar cookers, and solar air collectors [13].

Enhancement of the PCM thermal conductivity was the subject of several researchers' studies. Wang et al. [5] used different densities of compressed expanded natural graphite to enhance the thermal conductivity of neopentyl glycol for PCM thermal storage application. They reported that the thermal conductivities of the composites could be enhanced from 11 to 88 times compared with that of pure neopentyl glycol. Shi et al. [14] compared two enhancement methods to improve the thermal conductivity and shape stability of paraffin PCMs using exfoliated graphite nanoplatelets and graphene.

* Corresponding author. Tel.: +60 176135676; fax: +60 389214593.
E-mail addresses: abo_anas4@yahoo.com, abduljalil17@gmail.com (A.A. Al-Abidi).

0378-7788/$ – see front matter © 2013 Elsevier B.V. All rights reserved.
http://dx.doi.org/10.1016/j.enbuild.2013.09.007

Kurnia et al. [15] numerically investigated the different configurations of the PCM thermal storage (including the U-tube, U-tube with in line and staggered fins, and novel festoon design) to improve the heat transfer between the PCM and the HTF. Moreover, they used multi PCMs to enhance the heat transfer under different PCM arrangements. Tay et al. [16] investigated a new heat transfer-enhancement technique by implementing dynamic melting for a tube-in-tank thermal storage. They circulated melted PCM using pre-melt tubes in the frozen PCM. The result indicated that, for high- and low-temperature gradients, the average effectiveness increased between 33% and 89% and between 58% and 82%, respectively. Another technique to enhance the heat transfer in the PCM thermal storage by increasing the heat transfer area involves the use of a triplex tube heat exchanger (TTHX). Al-Abidi et al. [17] experimentally investigated the PCM melting process in the middle tube of TTHX. They studied three heating approaches to melt the PCM: inside heating method, outside heating method, and heating at both sides. The charging process totally depended on the solar heating. Temperature distributions in three directions were studied. They reported that heating both sides of the middle tube is preferable because low HTF inlet temperature is used, and the PCM melting time was reduced in contrast to those of the other methods.

The use of fins embedded in the PCM is considered the most efficient method to enhance the heat transfer in the PCM thermal storage and has been extensively investigated by researchers recently. This method is characterized by simplicity, efficiency, and ease in fabrication.

Tay et al. [18] compared different pin and fin configurations for the tube-coiled PCM thermal energy storage for heat transfer enhancement. The results indicated that the finned tube method was better than the pin method because of its average effectiveness as well as shorter phase-change duration. They concluded that the use of fins is a more effective heat transfer-enhancement technique for all shell-and-tube-type and tube-in-tank-type PCM thermal storage systems. Agyimen et al. [2,19] used a circular fin, longitudinal fin, and multitubes heat transfer enhancements to achieve the complete melting of erythritol as a PCM thermal storage to power an absorption-type air-conditioning system. The main objective of these techniques was to melt the PCM through the solar energy availability in Europeans countries where the sunshine is less than 8 h. They reported that the longitudinal fin and the multi-tubes thermal energy storage systems are suitable for charging and discharging in a concentric tube PCM system because they achieved the best charging performance with insignificant subcooling during discharge.

The different design parameters of vertically axial fins, such as the number of fins, fin length, fin thickness, and aspect ratio of the annular space, affect the time of solidification, solid mass fraction, and the total stored energy have been studied by Ismail et al. [20]. They reported that the annular space size, the radial length of the fins and the fins number have a strong effect on the time of complete phase change. A two-dimensional (2D) analytical model of the PCM solidification process in a shell-and-tube exchanger with radial fins was presented by Mosaffa et al. [21]. Two geometrical configurations (cylindrical and rectangular) with the same volume and heat transfer-surface area were compared for the PCM solidification process. The PCM solidified more quickly in the cylindrical shell than in the rectangular shell storage. In addition, the solid fraction of the PCM increased more quickly when the cell aspect ratio was small. Al-Abidi et al. [22] introduced external and internal fins to TTHX as a heat transfer-enhancement technique. They numerically investigated the effect of different design and operation parameters such as the fin length, fin thickness, number of fins, and PCM geometries, as well as the TTHX materials and Stefan number, on the melting process. The result indicated that the melting time for the eight-cell PCM unit geometries was reduced to 34.7% compared with that of the triplex tube without fins.

The time required to complete the PCM melting is an important factor in determining the amount of energy absorbed or released. On the other hand, the charging process depends on the HTF mass flow rate and inlet temperature. The effects of the non-steady state of the HTF inlet temperature and the mass flow rate on the thermal performance of the shell-and-tube PCM thermal storage were numerically analyzed by Tao and He [23]. The results showed that the PCM melting time decreases with the increase in the initial HTF inlet temperature and initial HTF inlet mass flow rate when the average inlet temperature and the average inlet mass flow are fixed within an hour. Ismail and Moraes [24] numerically and experimentally studied the effect of the PCM container materials, configuration, and dimensions on the PCM solidification to determine the time required for complete solidification.

The TTHX with a PCM in the middle tube can be used as thermal energy storage to increase the heat transfer area and improve the heat transfer process compared with the other heat exchanger configurations. In addition, the time required for the total melting/solidification decreases, and low inlet HTF temperatures are required to charge the PCM. Welding of different fins at the middle and inner tube enhances the heat transfer process, and more time reduction can be achieved.

The experiment in our present work primarily studied the thermal performance of a TTHX with internal and external fins. The experiment examined the PCM charging process under steady and non-steady heat transfer-inlet temperature and the influence of the mass flow rates on the PCM melting. The PCM solidification process was investigated under different mass flow rates. The experiment was performed to reduce the time required to complete the PCM melting using the available solar energy in the application location. The other important objective of this experiment was to determine the influence of the operation parameters on the charging process to develop a control operation strategy that can achieve complete melting of the PCM by the available sunlight, especially in locations where the sky is often overcast. The stored energy delivers the thermal energy that can power a liquid desiccant air-conditioning system.

2. Experimental test and procedure

2.1. PCMs

The operating temperature required for the regeneration of the liquid desiccant air conditioning is the basis in the selection of the PCM, which is in the range from 65 °C to 70 °C. The RT 82 paraffin (RUBITHERM GmbH-Germany) with an 82 °C melting temperature satisfies the minimum temperature required for the liquid desiccant cooling system. The thermophysical properties of RT82 as reported by the manufacturer and independently investigated by the authors have been reported in [17].

2.2. Experimental apparatus

A thermal energy storage system using the triplex concentric tube heat exchanger with internal and external fins was fabricated to investigate the heat transfer enhancement on the thermal performance from the use of the fins. Fig. 1 shows the schematic diagram of the experimental apparatus that includes three main circuits: the main heating, the charging, and the discharging circuits. The main heating circuit contained an evacuated-tube solar collector, a main circulation pump, and two storage tanks with an electric heater. The charging circuit consisted of a charging circulation pump, a PCM thermal storage with fins, and the charging storage

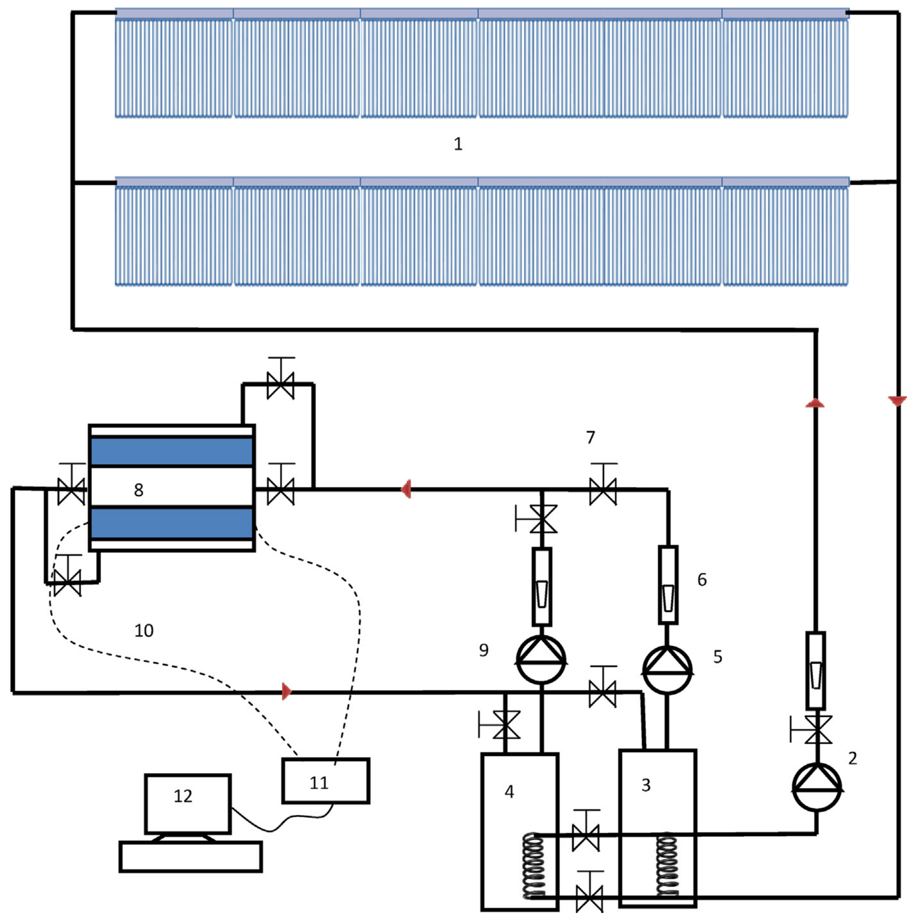

Fig. 1. Schematic diagram of the experimental apparatus which includes an evacuated tube solar collector (1), main heating circulation pump (2), charging storage tank (3), discharging storage tank (4), charging circulation pump (5), rotameter to measure the flow rate (6), manual shut off valve (7), a triplex concentric tube's heat exchanger (8), discharging circulation pump (9), thermocouples (10), data logger (11) and personal computer (12).

tanks. The discharging circuit comprised the discharging circulation pump, the PCM thermal storage, and the discharging storage tanks. Fig. 2 shows the PCM thermal storage section that includes a TTHX that comprises three horizontally mounted concentric tubes with lengths of 500 mm. The inner tube has a radius (*ri*) of 25.4 mm and a thickness of 1.2 mm. The middle tube has a radius (*rm*) of 75 mm, and the outer tube has a radius (*ro*) of 100 mm. Both tubes are 2 mm thick. All pipes were made of copper to ensure high thermal conductivity. The inner tube was extended to approximately 300 mm from the entrance to ensure a fully developed dynamic flow. Two tubes with a 32 mm diameter were welded eccentrically to the outer tube from above and below the entrance and exit of the HTF to deliver the hot water in and out of the outer tubes, as shown in Fig. 2. The inner and outer tubes were used to hold the HTF (water), and the middle tube was filled with 5.6 kg of liquid PCM (RT 82). Four longitudinal fins (fin pitch = 42 mm, length = 480 mm, and thickness = 1 mm) were welded onto each of the inner and middle tubes to improve the heat transfer in the PCM thermal storage. A short tube with a diameter of 32 mm was connected to the middle tube from the two faces, which enables the change in the PCM. Two copper end plates with a 2 mm thickness were welded to the tubes. The data monitoring system comprised the K-type thermocouples

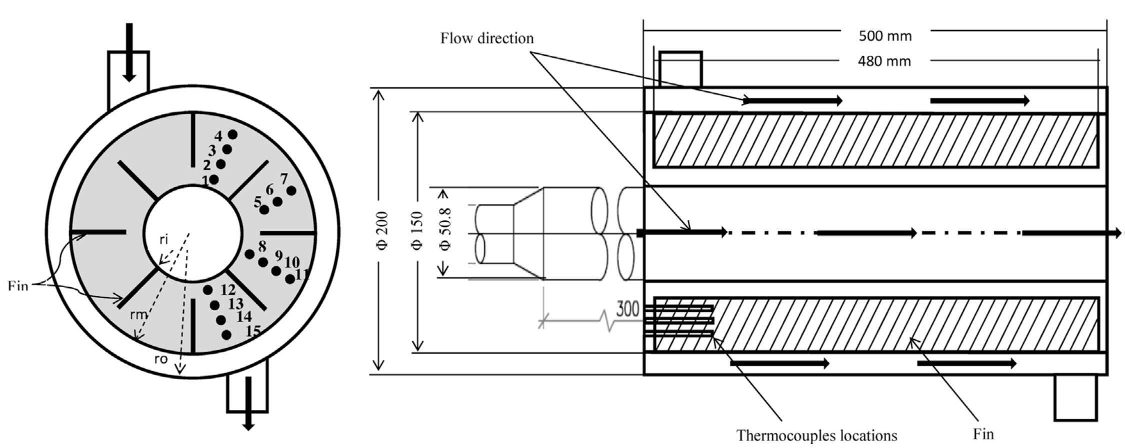

Fig. 2. Schematic diagram of the TTHX; (a) cross section of TTHX, (b) longitudinal section of TTHX.

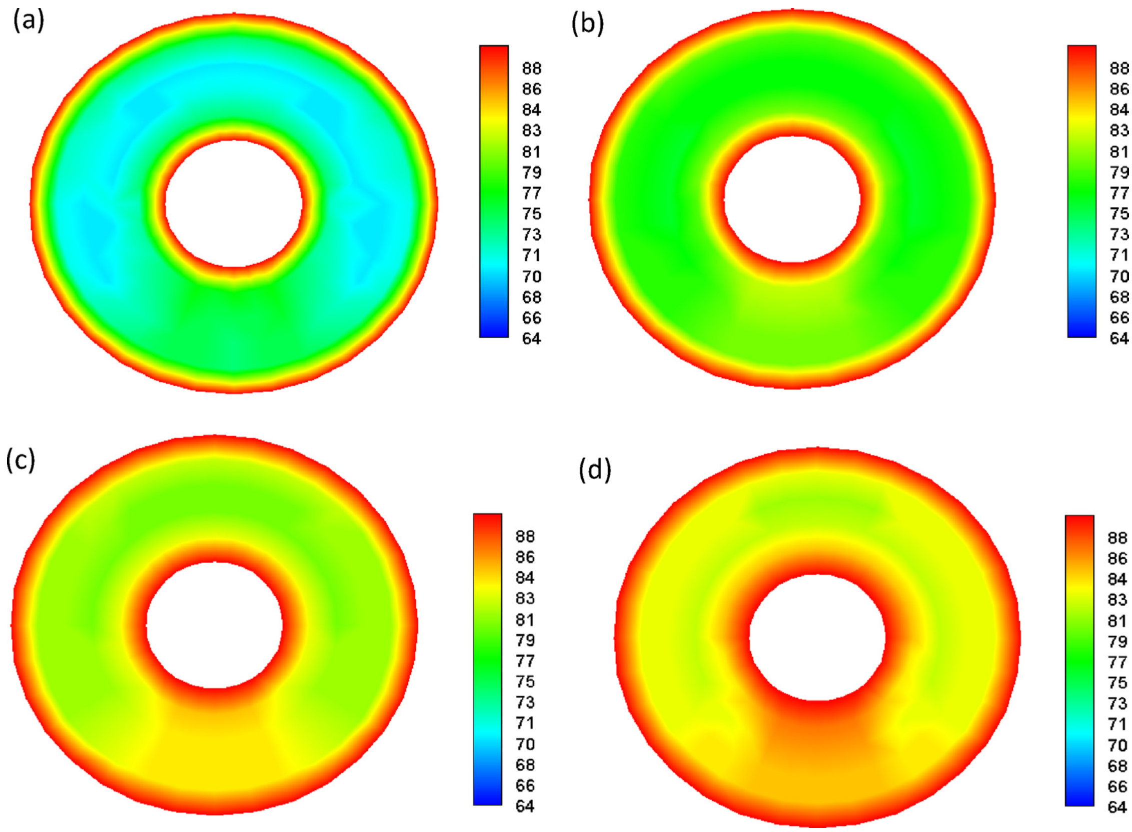

Fig. 3. Temperature contour of the PCM during melting, average charging temperature ($Ti = 90\,^{\circ}$C); (a) $t = 15$ min, (b) $t = 30$ min, (c) $t = 45$ min, (d) $t = 60$ min.

(measured at 0.5% accuracy), a data logger, and a personal computer to measure the temperature in the PCM thermal storage. The HTF flow rate was measured by a rotameter (measured at 5% accuracy).

Fifteen thermocouples were installed in the PCM at 10 mm intervals, fitted in the radial and different angular directions and located 100 mm from the entrance of the HTF, as shown in Fig. 2. Two thermocouples were also installed at the inlet and outlet of the HTF tube to measure the HTF inlet and outlet temperatures. The PCM thermal storage was wrapped with a 70 mm-thick glass wool insulation to decrease the heat loss and achieve an adiabatic surface.

The hot water used for the charging and discharging process was delivered from the central heating station of the Green Technology Park at Solar Research Energy Institute, National University of Malaysia. This heating station is tapped to deliver the hot water requirements of various solar thermal systems. The central heating station comprises 300 evacuated-tube solar collectors with three 200 L storage tanks. Two of these storage tanks were used for the current application: one for charging and the other for discharging. The charging of the thermal storage was facilitated by the heat delivered by the main circulation pump from the solar collector to the storage tank. As the temperature of the storage tank reached the PCM melting temperature, the charging pump was activated to deliver hot water to melt the PCM in the thermal storage. For the non-steady HTF inlet temperature, the inlet temperatures were varied relative to the solar radiation, whereas the steady state HTF inlet temperature was operated by thermostat-controlled electrical heating, which maintained the required set temperature. The PCM freezing process started when the entire PCM melted. The temperature of the discharging storage tank was maintained at 68 °C, considered the minimum temperature to power the liquid desiccant air conditioning. The initial temperature of the PCM was set at ambient temperature.

3. Experimental results

3.1. Melting with steady-state HTF inlet temperature

Different experimental studies were conducted to charge the PCM thermal storage with steady state HTF inlet temperature. The charging process to melt the PCM depended on the electrical heat sources. Heating up of the storage tank was done by solar heating source until the required temperature was achieved. Then, the electric heater, controlled by a thermostat, was run to maintain a constant inlet temperature. In some experiments, the inlet temperature fluctuated (±1.5 °C) from the set point temperature. A number of experiments have been conducted to study the effect of the operating parameters on the melting time of the thermal storage, such as the HTF inlet temperature variation and the mass flow rate. Temperature readings of the 15 thermocouples immersed in the PCM thermal storage were taken 100 mm from the entrance.

3.1.1. Temperature contour of the PCM

The temperature contours of the PCM thermal energy storage at $t = 15$ min, $t = 30$ min, $t = 45$ min, and $t = 60$ min from a selection of the charging experiments ($Ti = 90\,^{\circ}$C, $m = 8$ kg/min) are shown in Fig. 3. The temperature readings were based on the thermocouples imbedded in the PCM thermal storage entrance and from linear interpolation between points [1,25]. During 15 min of charging, a thin liquid formed in the narrow melt layer beside the inner and the outer tubes. The average temperature at the upper region was lower than that at the bottom region for the PCM thermal storage, which was between 68 °C and 72 °C. After 30 min of charging, the thin liquid expanded, whereas the temperature distributions in the PCM remained uniform. The temperature distributions in the PCM were equal, which were between 73 °C and 80 °C. As time progressed, the differences in the temperature between the bottom and top regions

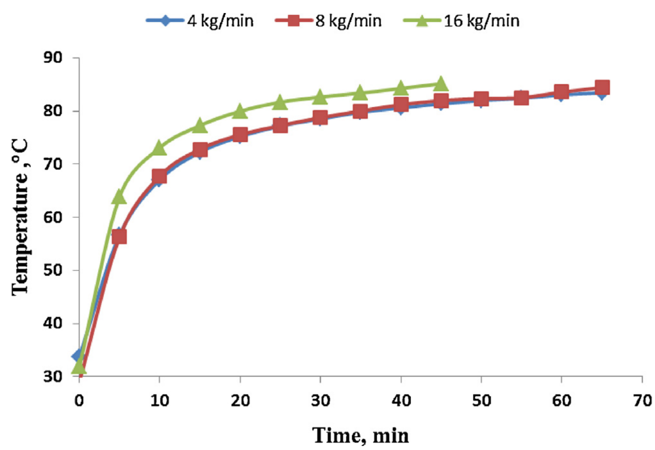

Fig. 4. HTF mass flow rate effect on the PCM melting time.

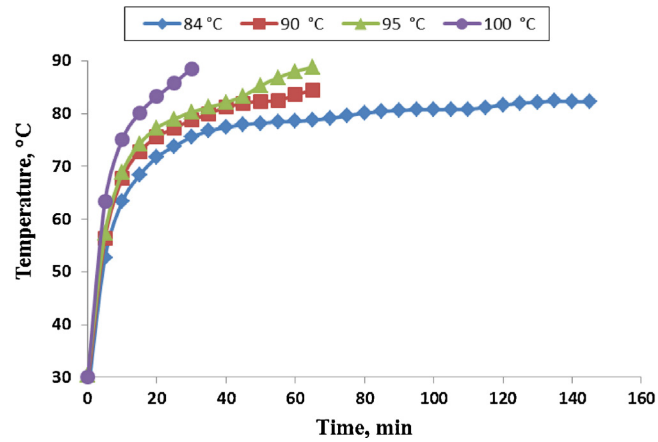

Fig. 5. HTF inlet temperature effect on the PCM melting time.

reappeared in which that at the bottom zone was higher, which was attributed to a good thermal diffusion in the bottom part, whereas the upper part was affected by the entrance disturbance. The flow was disturbed by changing the flow path from the 32 mm-inlet pipe to the outer tube. The other source that affected the heat diffusion in this part was the location of the outer tube inlet pipe, which was not centered but was soldered at the left side, as shown in Fig. 2. The melting process continued until the entire PCM melted.

3.1.2. Effect of mass flow

Different mass flow rates of the HTF were used to study their effect on the PCM melting process. All experiments were conducted using a constant HTF temperature of 90 °C. Fig. 4 shows the average temperature versus time for the HTF mass flow rates of 4, 8, and 16 kg/min. The average PCM temperatures were equal for the 4 and 8 kg/min HTF flow rates, attributed to the still flow in the laminar flow. A good enhancement was apparent when the flow rate increased to 16 kg/min, which is considered a turbulent flow and regarded as good for the heat transfer process. The charging time decreased by 58%. We can conclude that the influence when the mass flow rate changed from 4.0 to 8.0 is insignificant, whereas the melting rate accelerated when the flow rate increased to 16.0 kg/min.

3.1.3. Effect of HTF inlet temperature

The charging of the PCM under different HTF inlet temperatures was performed at an 8 kg/min mass flow rate. Various HTF inlet temperatures of 85, 90, 95, and 100 °C to melt the PCM were investigated. The selection of these temperature values was based on the minimum temperature required to achieve PCM melting, which was above the PCM melting temperature and the maximum temperature using water as HTF. Fig. 5 shows the average PCM temperature versus time for HTF inlet temperatures of 85, 90, 95, and 100 °C. Complete melting occurred when the HTF inlet temperature was 90, 95, and 100 °C. The 85 °C HTF inlet temperature did not achieve entire PCM melting, and the melting time was extended to 170 min. No significant difference was observed between 90 and 95 °C, possibly because of the fluctuation in the inlet temperature at 95 °C. The total melting times of the PCMs were reduced to 86% by increasing the HTF inlet temperature from 85 °C to 100 °C.

3.2. Melting with non-steady state HTF inlet temperature

Most solar energy-application systems operate under a non-steady state condition. Thus, the PCM thermal storage was investigated by varying the HTF inlet temperature because of the dependence of the charging process on the solar energy sources. Fig. 6 shows the HTF inlet temperatures (charging temperatures) versus time for different mass flow rates of 4, 8, 16, and 24 kg/min to charge the thermal storage. The initial charging temperature for the mass flow rates of 4, 8, 16, and 24 kg/min were 82, 83.4, 87.7, and 88.6 °C, respectively. The charging temperature at the mass flow rates of 4 and 24 kg/min increased with time, whereas the mass flow rate of 16 kg/min increased in the beginning of the charging, remained steady with the charging temperature, and increased again until the entire PCM melted. Fluctuation in the charging temperature occurred at the mass flow rate of 8 kg/min.

Fig. 7 shows the average PCM temperature versus time for the non-steady state mass flow rates of 4, 8, 16, and 24 kg/min. The average PCM temperature at 4 and 8 kg/min were the same for the 40 min of charging. Then, the PCM average temperature at 4 kg/min increased as the charging temperature increased, whereas the 8 kg/min flow rate consumed more time in melting the PCM because its charging temperature fluctuated according to the solar radiation. The average PCM temperatures at the 16 and 24 kg/min mass flow rates were equal until the melting process was completed, whereas the charging temperatures were different. Therefore, we can conclude that the effect of the mass flow rate was insignificant relative to that of the charging temperature. For thermal energy storage by solar energy, a control device in the charging circuit is recommended because the solar radiation fluctuation leads to different HTF inlet temperatures. When the HTF temperature decreases, the mass flow rate should be increased, and vice versa to maintain steady state condition for charging and fast melting.

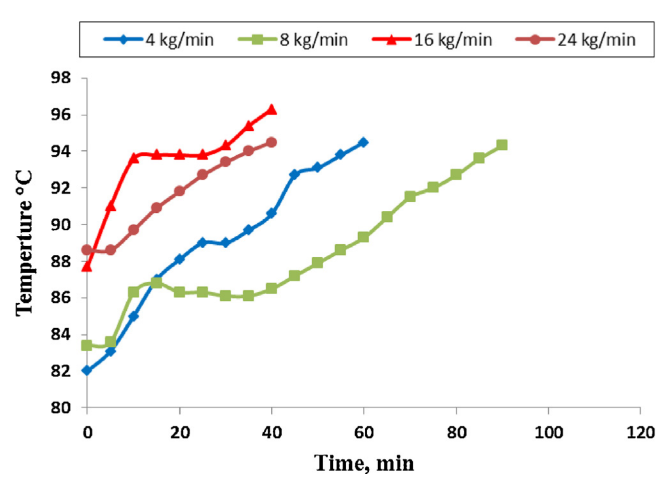

Fig. 6. HTF inlet temperature (charging temperature) of the thermal storage.

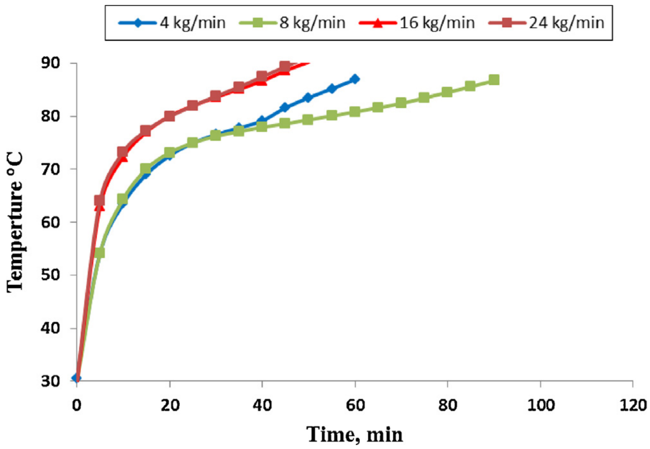

Fig. 7. PCM average temperature of the thermal storage.

3.3. Solidification process

3.3.1. Temperature contour of the PCM

The solidification process starts directly after the entire PCM melting. Fig. 8 shows the temperature contours at 15, 30, 45, and 60 min from a selection of discharge experiments ($Ti = 68\,^{\circ}C$; $m = 8$ kg/min). The temperature readings depended on the same thermocouple location mentioned in the melting process and the interpolation between these points. At the initial time of solidification (15 min), the entire PCM was in the mushy zone which is the region between the liquidus and solidus isotherms, where solid and liquid coexist in thermal equilibrium, the temperature readings were between 73 and 80 °C. The average PCM temperature was not uniform, and two solid layers were formed near the inner and outer tubes. The average temperature in the upper part of the storage was lower than those at the other regions, which may be attributed to the trapped air in this part during the filling of the storage with liquid PCM and the formation of void during the freezing process.

As time progressed, the average temperature became uniform except for the upper part at $t = 45$ min. The solidification front increased at the lower part of the inner tube and the upper part of the thermal storage, which indicated a mushy layer of the PCM trapped between the inside and outside solid layers. This layer required more time to solidify because as the solid layer increased, the thermal resistance increased. The entire PCM solidified after 60 min of freezing.

3.3.2. Effect of the flow rate

To study the effect of the mass flow rate on the solidification processes, Fig. 9 shows the experimental data of the PCM freezing under different mass flow rates of 4, 8, and 16 kg/min. The solidification rate increased as the mass flow rate increased, attributed to the improvement in the heat transfer. The determination of the HTF flow rate during the solidification process depends on the load mass flow rate requirement.

3.4. Radial and angular temperature variation for thermal storage

In this study, 2D directional measurements along the radial and angular directions were considered to investigate the temperature variation for the thermal storage. The radial distance extends from the outer surface of the inner tube to the inner surface of the middle tube. The angular direction starts from 0° clockwise to 157.5°, as shown in Fig. 10. Figs. 11 and 12 show the average temperature variations along the radial and angular directions for

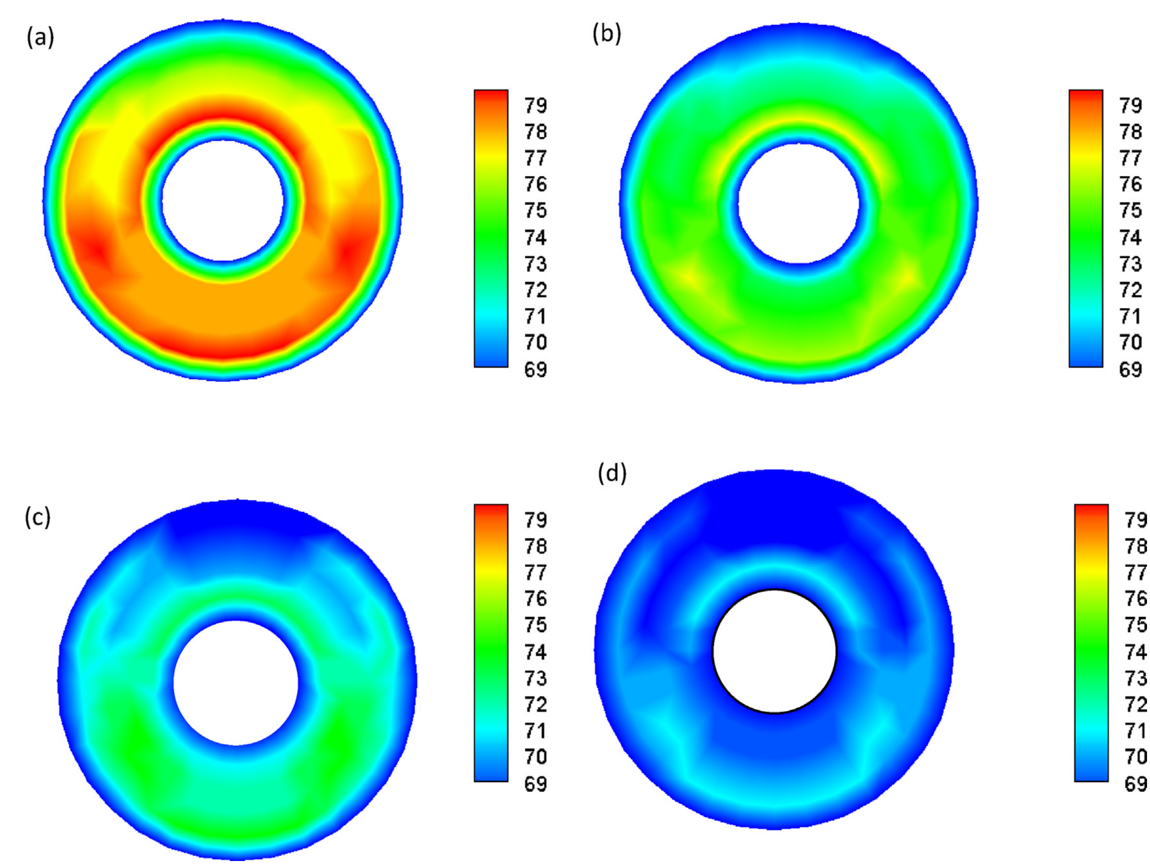

Fig. 8. Temperature contour of the PCM during solidification, average discharging temperature ($Ti = 68\,^{\circ}C$); (a) $t = 15$ min, (b) $t = 30$ min, (c) $t = 45$ min, (d) $t = 60$ min.

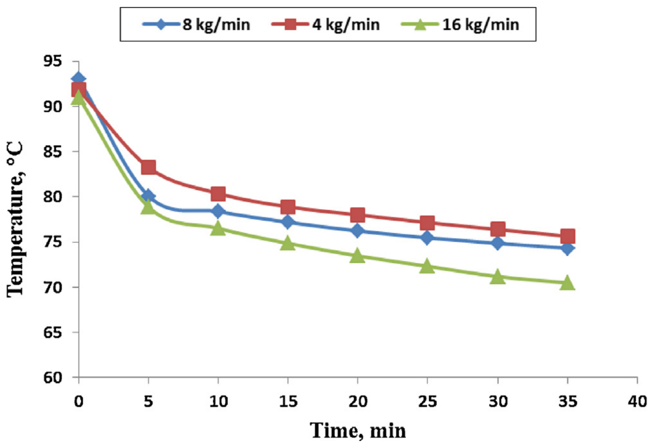

Fig. 9. HTF mass flow rate effect on the PCM solidification time.

the melting and solidification processes. These averages were collected from different thermocouple readings in different locations at the thermal storage entrance. Radial average temperature variation was observed in the thermocouples located within the same distance from the inside tubes (r = 10 mm, r = 20 mm, r = 30 mm, and r = 40 mm). The angular average temperature-variation readings were taken from thermocouples at the same angles (22.5, 67.5, 112.5, and 157.5°) as shown in Fig. 10.

3.4.1. Radial and angular temperature variations in melting process

The temperature variation along the radial direction during the melting process is shown in Fig. 11(a), which shows the average temperature versus time at different melting times. The melting front appeared at different times. The temperature differences between the four distances were clearly observed during the early stage after 10 min of melting. The highest temperature was at r = 10 mm, followed by r = 40 mm. This result was attributed to the heat transfer from the inner and outer tubes in which the conduction mechanism dominates the heat transfer process between the PCM and the HTF. No significant difference in the temperature was observed between r = 20 mm and r = 30 mm that followed the two positions near the tubes. As time progressed, the temperature in the inner region where r = 10 mm continued to increased and was considered higher than those of the other regions, whereas those

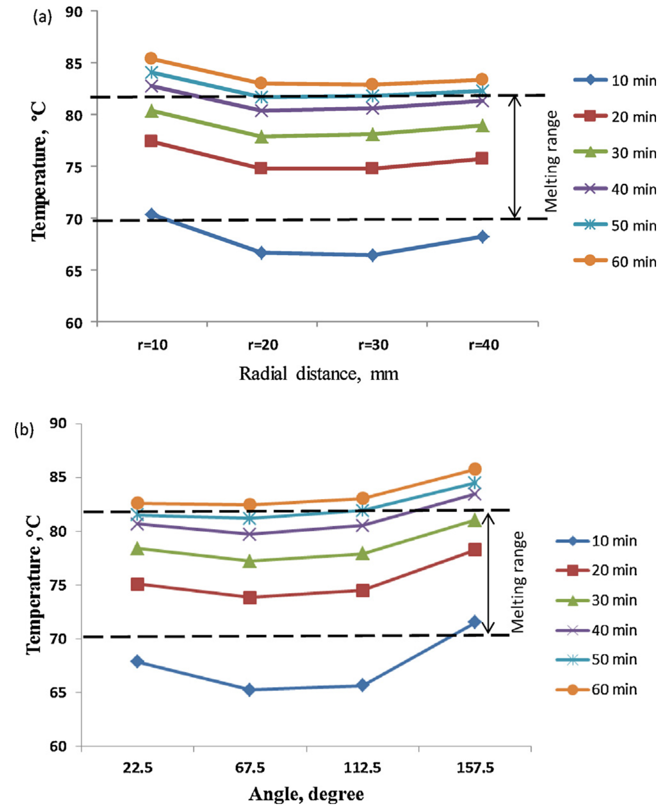

Fig. 11. Average temperatures recorded in the thermal storage during the melting process, (a) radial direction, (b) angular direction.

at r = 20 mm and r = 30 mm were approximately equal at t = 20 min. At the end of the melting process, the average temperature at r = 10 mm was high due to the early appearance effect of the natural convection until the completion of the melting process, whereas those at the three distances of r = 20 mm, r = 30 mm, and r = 40 mm were equal, and the entire PCM melted after 60 min.

The average PCM temperature along the angular direction at different times of melting is shown in Fig. 11(b). After 10 min of heating, the average temperature at θ = 157.5°, located at the bottom of the thermal storage, was higher than that at the other directions due to the good thermal diffusion, followed by θ = 22.5°

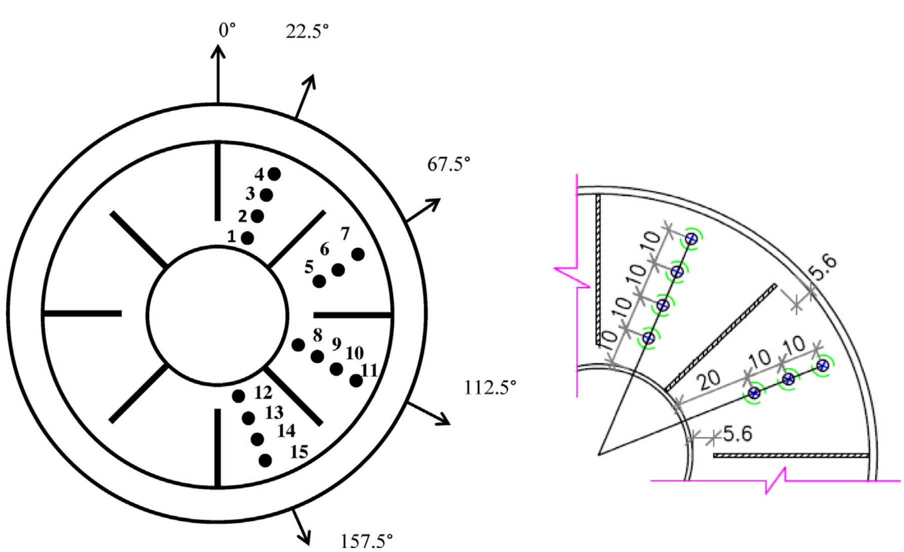

Fig. 10. Thermocouple locations along the radial and angular locations in the PCM.

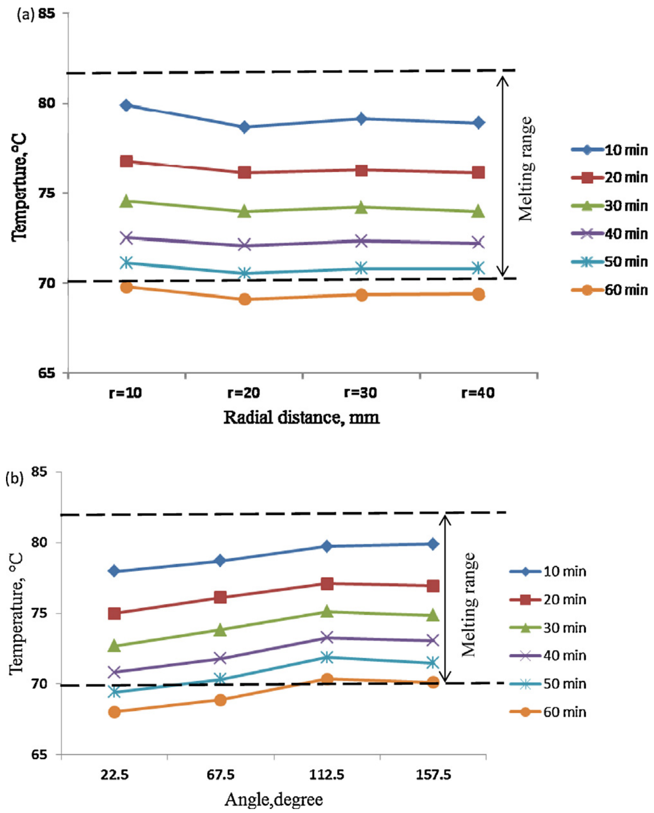

Fig. 12. Average temperatures recorded in the thermal storage during the solidification process, (a) radial direction, (b) angular direction.

at the top side of the thermal storage. The average temperature occurred at $\theta = 67.5^\circ$ and $\theta = 112.5^\circ$ were less than $\theta = 22.5^\circ$, whereas no significant difference in the average temperature was observed at $\theta = 67.5^\circ$ and $\theta = 112.5^\circ$. This condition remained until time $t = 50$ min when the average temperature at $\theta = 112.5^\circ$ was higher than that at $\theta = 22.5^\circ$. By the end of the melting process, the average temperatures at the three angular directions $\theta = 22.5^\circ$, $\theta = 67.5^\circ$, and $\theta = 112.5^\circ$ were equal, whereas that at $\theta = 157.5$ was higher, which is attributed to the thermal diffusion and natural convection because the PCM melting point was achieved early in this side compared with those in the other directions.

3.4.2. Radial and angular temperature variations in solidification process

The average temperature along the radial direction during the PCM solidification at different times is shown in Fig. 12(a). The sensible cooling of the PCM drastically decreased. After 10 min of freezing, the entire PCM was in the mushy zone (transition phase). The cooling trend was the same at any given time; the cooling rate was higher in the outer tube than that in the inner tube due to the increase in the outer tube surface heat transfer area. The cooling rate decreased as time progressed because of the increase in the thermal resistance owing to the increase in the solid layer front. The entire PCM solidified after 60 min of freezing.

Fig. 12(b) shows the average PCM temperature during the solidification process along the angular direction at different times. The solidification rate decreased as the angle increased from 22.5° to 112.5°. The average PCM temperature at $\theta = 112.5^\circ$ was the same as that at $\theta = 157.5^\circ$ at any time, and the cooling rate at $\theta = 22.5^\circ$ was higher due to the effect of air in the upper zone on the thermal storage. The average PCM temperature at $\theta = 22.5^\circ$ was almost the same as that of the HTF after 60 min of freezing, whereas the PCM has a lower limit in the transition range.

4. Conclusion

The melting and solidification processes in a TTHX with internal and external fins have been experimentally investigated. Different mass flow rates for the PCM transition process were studied. The experiments were performed under steady and non-steady state inlet HTF for the melting process. The temperature gradients along the angular and radial directions were investigated. The results indicated that the HTF inlet temperature has a significant effect on the melting process compared with the mass flow rates. A control strategy is recommended to achieve complete melting of the PCM when the energy source depends on solar energy.

References

[1] F. Agyenim, N. Hewitt, The development of a finned phase change material (PCM) storage system to take advantage of off-peak electricity tariff for improvement in cost of heat pump operation, Energy and Buildings 42 (9) (2010) 1552–1560.
[2] F. Agyenim, P. Eames, M. Smyth, Heat transfer enhancement in medium temperature thermal energy storage system using a multitube heat transfer array, Renewable Energy 35 (1) (2010) 198–207.
[3] C.W. Robak, T.L. Bergman, A. Faghri, Enhancement of latent heat energy storage using embedded heat pipes, International Journal of Heat and Mass Transfer 54 (15) (2011) 3476–3484.
[4] R. Velraj, R.V. Seeniraj, B. Hafner, C. Faber, K. Schwarzer, Heat transfer enhancement in a latent heat storage system, Solar Energy 65 (3) (1999) 171–180.
[5] X. Wang, Q. Guo, Y. Zhong, X. Wei, L. Liu, Heat transfer enhancement of neopentyl glycol using compressed expanded natural graphite for thermal energy storage, Renewable Energy 51 (2013) 241–246.
[6] H.A. Adine, H. El Qarnia, Numerical analysis of the thermal behaviour of a shell-and-tube heat storage unit using phase change materials, Applied Mathematical Modelling 33 (4) (2009) 2132–2144.
[7] A.H. Mosaffa, C.A. Infante Ferreira, F. Talati, M.A. Rosen, Thermal performance of a multiple PCM thermal storage unit for free cooling, Energy Conversion and Management 67 (2013) 1–7.
[8] A.A. Al-Abidi, S. Bin Mat, K. Sopian, M. Sulaiman, C. Lim, A. Th, Review of thermal energy storage for air conditioning systems, Renewable and Sustainable Energy Reviews 16 (8) (2012) 5802–5819.
[9] M.M. Farid, A.M. Khudhair, S.A.K. Razack, S. Al-Hallaj, A review on phase change energy storage: materials and applications, Energy Conversion and Management 45 (9/10) (2004) 1597–1615.
[10] H. Hu, S.A. Argyropoulos, Mathematical modelling of solidification and melting: a review, Modelling and Simulation in Materials Science and Engineering 4 (1996) 371–396.
[11] A.M. Khudhair, M.M. Farid, A review on energy conservation in building applications with thermal storage by latent heat using phase change materials, Energy Conversion and Management 45 (2) (2004) 263–275.
[12] C. Zhang, Y. Chen, L. Wu, M. Shi, Thermal response of brick wall filled with phase change materials (PCM) under fluctuating outdoor temperatures, Energy and Buildings 43 (12) (2011) 3514–3520.
[13] A.A. Al-Abidi, S.B. Mat, K. Sopian, M.Y. Sulaiman, A.T. Mohammed, CFD applications for latent heat thermal energy storage: a review, Renewable and Sustainable Energy Reviews 20 (2013) 353–363.
[14] J.-N. Shi, M.-D. Ger, Y.-M. Liu, Y.-C. Fan, N.-T. Wen, C.-K. Lin, N.-W. Pu, Improving the thermal conductivity and shape-stabilization of phase change materials using nanographite additives, Carbon 51 (0) (2013) 365–372.
[15] J.C. Kurnia, A.P. Sasmito, S.V. Jangam, A.S. Mujumdar, Improved design for heat transfer performance of a novel phase change material (PCM) thermal energy storage (TES), Applied Thermal Engineering 50 (1) (2013) 896–907.
[16] N.H.S. Tay, F. Bruno, M. Belusko, Experimental investigation of dynamic melting in a tube-in-tank PCM system, Applied Energy 104 (0) (2013) 137–148.
[17] A.A. Al-Abidi, S. Mat, K. Sopian, M.Y. Sulaiman, A.T. Mohammad, Experimental study of PCM melting in triplex tube thermal energy storage for liquid desiccant air conditioning system, Energy and Buildings 60 (0) (2013) 270–279.
[18] N.H.S. Tay, F. Bruno, M. Belusko, Comparison of pinned and finned tubes in a phase change thermal energy storage system using CFD, Applied Energy 104 (0) (2013) 79–86.
[19] F. Agyenim, P. Eames, M. Smyth, A comparison of heat transfer enhancement in a medium temperature thermal energy storage heat exchanger using fins, Solar Energy 83 (9) (2009) 1509–1520.
[20] K.A.R. Ismail, C.L.F. Alves, M.S. Modesto, Numerical and experimental study on the solidification of PCM around a vertical axially finned isothermal cylinder, Applied Thermal Engineering 21 (2001) 53–77.
[21] A.H. Mosaffa, F. Talati, Basirat Tabrizi r H., M.A. Rosen, Analytical modeling of PCM solidification in a shell and tube finned thermal storage for air conditioning systems, Energy and Buildings 49 (2012) 356–361.
[22] A.A. Al-Abidi, S. Mat, K. Sopian, M.Y. Sulaiman, A.T. Mohammad, Internal and external fin heat transfer enhancement technique for latent heat thermal energy storage in triplex tube heat exchangers, Applied Thermal Engineering 53 (1) (2013) 147–156.

[23] Y.B. Tao, Y.L. He, Numerical study on thermal energy storage performance of phase change material under non-steady-state inlet boundary, Applied Energy 88 (11) (2011) 4172–4179.
[24] K.A.R. Ismail, R.I.R. Moraes, A numerical and experimental investigation of different containers and PCM options for cold storage modular units for domestic applications, International Journal of Heat and Mass Transfer 52 (19/20) (2009) 4195–4202.
[25] F. Agyenim, P. Eames, M. Smyth, Experimental study on the melting and solidification behaviour of a medium temperature phase change storage material (Erythritol) system augmented with fins to power a LiBr/H_2O absorption cooling system, Renewable Energy 36 (2011) 108–117.